Supporting Information

Rationally Designed Mn_2O_3@$ZnMn_2O_4$/C Core-shell Hollow Microspheres for Aqueous-based Zinc Ion Batteries

Zhan Gao[a], Guoge Lu[a], Liucheng Cao[a], Zongxiu Zhu[a], Yingxin Li[a], Fuxiang Wei[a,b,*], Zhe Ji[a*], Yanwei Sui[a,b], Jiqiu Qi[a,b], Qingkun Meng[a,b], Yaojian Ren[a,b]

[a] *School of Materials and Physics, China University of Mining & Technology, Xuzhou, 221116, PR China*

[b] *The Jiangsu Province Engineering Laboratory of High Efficient Energy Storage Technology & Equipments under, China University of Mining & Technology, Xuzhou, PR China*

[*] *Corresponding author. School of Materials and Physics, China University of Mining & Technology, 1, university road, Xuzhou, 221116, PR China. E-mail address: weifuxiang2001@163.com (F. Wei), jizhe@cumt.edu.cn (Z. Ji).*

Electrochemical Characterizations

The Mn_2O_3@$ZnMn_2O_4$/C electrode was prepared by stirring slurry of active material (70 wt %), acetylene black (20 wt %) and polytetrafluoroethylene (10 wt %). The slurry was then coated on 0.02 mm thick titanium foil with a square coater and dried in an oven overnight at 70 °C. After drying, the titanium foil coated with active material was cut into 1.4 cm diameter discs (the loading of active material on titanium foil is about 1 mg cm^{-2}). CR2025 coin cells were assembled with the cathode of Mn_2O_3@ZnMn2O4/C electrode, the anode of zinc foil, 2 M $ZnSO_4$ + 0.1 M $MnSO_4$ electrolyte and glass fiber separator. The GCD curves of samples were performed by a battery tester (Land CT2001A system). Cyclic voltammetry (CV) tests were conducted by an electrochemical workstation (Gamry, American) with a voltage window from 0.8 V to 2.0 V at the scan rate of 0.2~1.0 mV s^{-1} and the electrochemical impedance spectroscopy (EIS) tests were performed on an electrochemical workstation (Gamry, American) at a frequency range from 100 kHz to 0.01 kHz.

Materials Characterization

The morphologies and structures of the as-prepared samples were characterized by scanning electron microscopy (SEM, SU8010) and transmission electron microscopy (TEM, Tecnai G2 F20). The crystal structure and phase composition were analyzed by X-ray diffraction (XRD, Bruker D8) with Cu Kα radiation between 10° and 80°. The chemical states of samples were determined by X-ray photoelectron spectroscopy (XPS, ESCALAB 250Xi). The pore distribution was characterized by isothermal N_2 adsorption/desorption using an automated adsorption apparatus (3Flex) at 77.3 K, and the specific surface area was calculated based on the BET (Brunauer-Emmett-Teller) equation. The thermal behaviors of $MnCO_3$@ZIF-8 microspheres were furtherly studied by Thermogravimetric Analysis (TG) using TA Instruments.

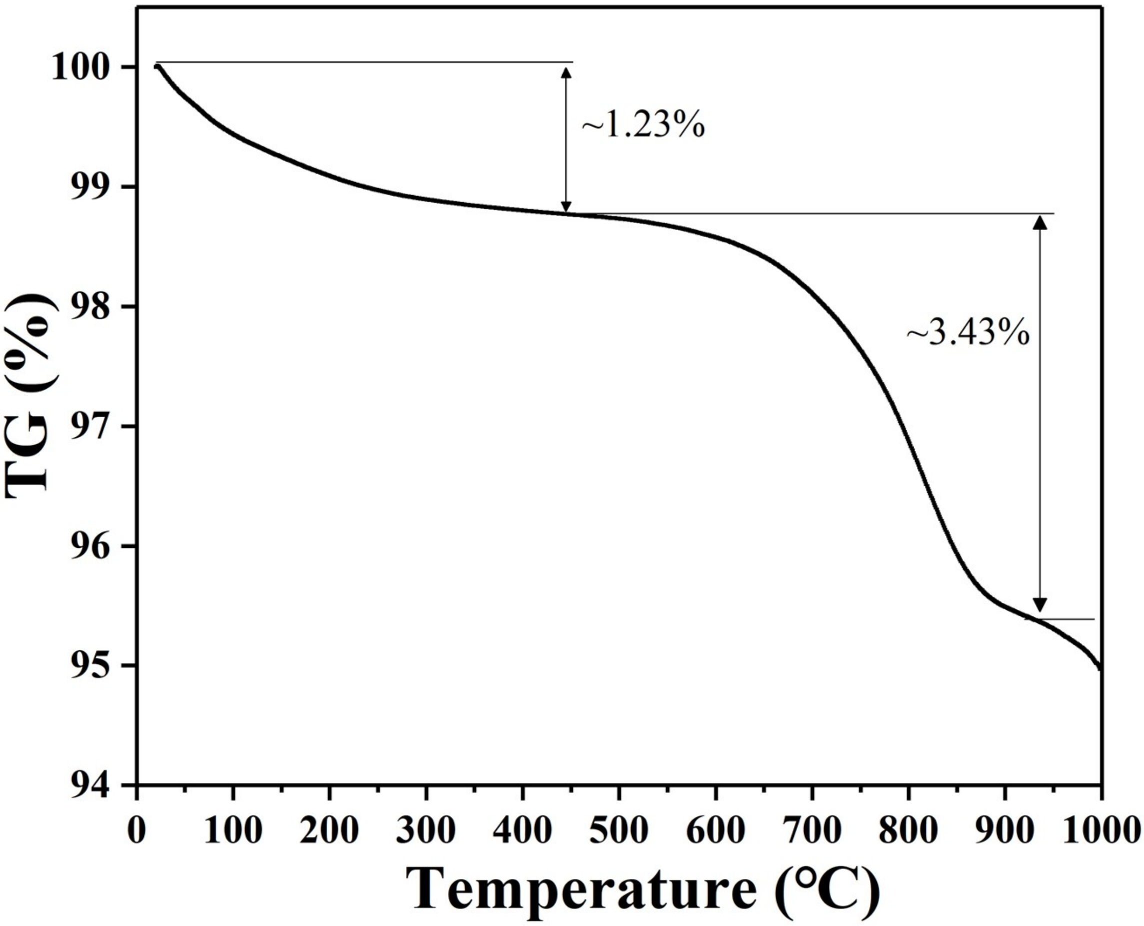

Fig. S1. The TG curve of Mn_2O_3@$ZnMn_2O_4$/C.

At beginning, the weight loss of samples (1.23 wt%) occurred at low temperature, corresponding to the removal of the physically and chemically adsorbed water. In terms of carbon, a sharp weight loss (3.43 wt%) from 450 °C to 930 °C can be easily seen in TG curve, which is ascribed to the oxidation of carbon. Therefore, the carbon content in Mn_2O_3@$ZnMn_2O_4$/C could be estimated as around 3.43 wt%.

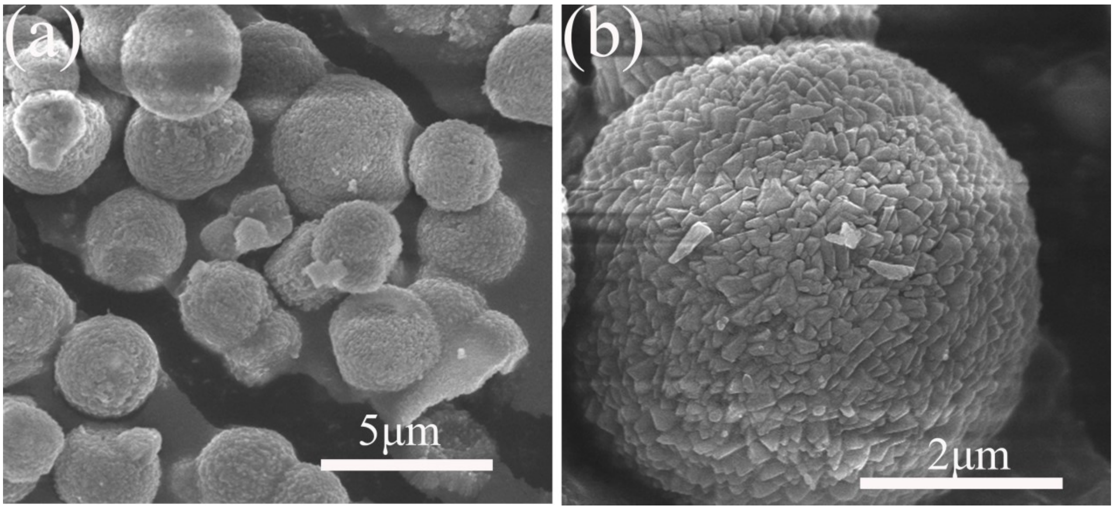

Fig. S2. (a, b) SEM images of $MnCO_3$

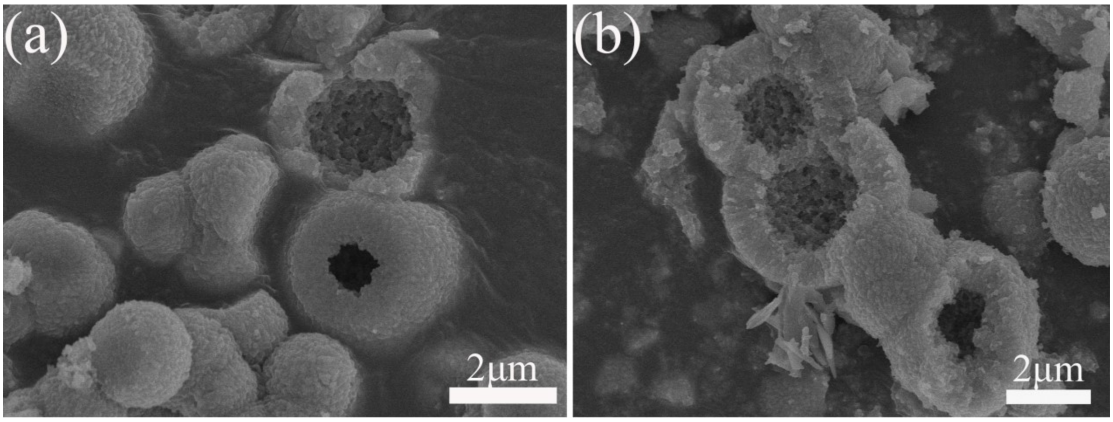

Fig. S3. (a, b) SEM images of broken Mn_2O_3@$ZnMn_2O_4$/C microspheres

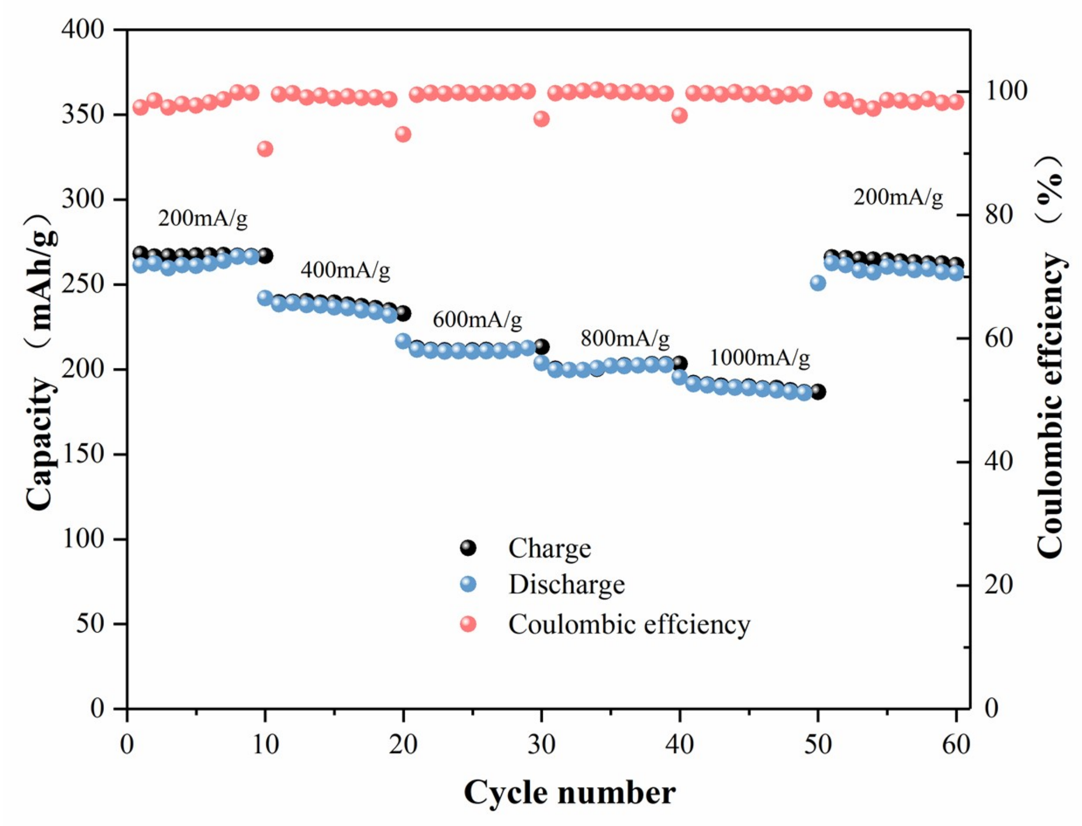

Fig. S4. Rate performance at different current densities of 200-1000 mA g^{-1} of the Mn_2O_3@$ZnMn_2O_4$/C cathode after cycling.

The rate performance of Mn_2O_3@$ZnMn_2O_4$/C after cycling was also been tested (Fig. S4), and achieved the discharge capacity of 266.1, 231.8, 212.4, 202.5 and 186.0 mAh g^{-1} at the current density of 200, 400, 600, 800 and 1000 mA g^{-1}, respectively.

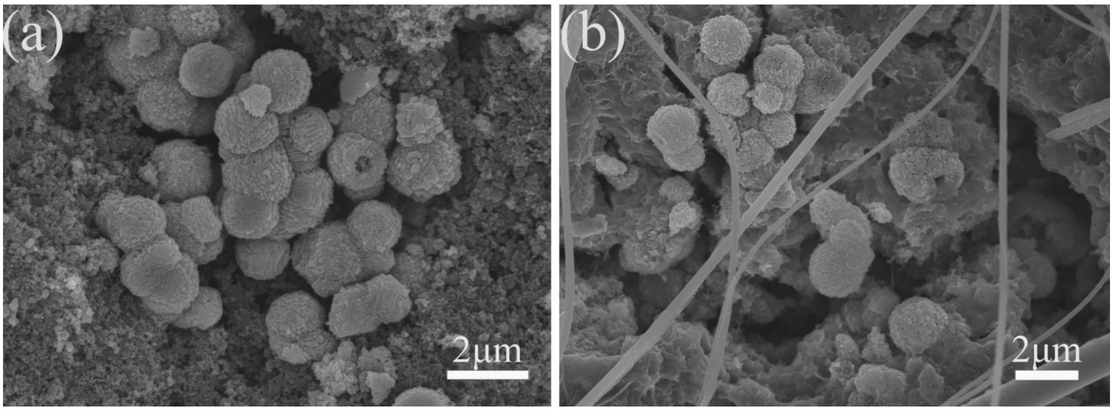

Fig. S5. SEM images of Mn_2O_3@$ZnMn_2O_4$/C electrode (a) Pristine electrode; (b) After cycling at 1000 mA g^{-1} for 700 times

To further confirm the integrity of the structure after cycling. The morphology of Mn_2O_3@$ZnMn_2O_4$/C electrode before and after cycling has also been studied. As shown in Fig. S5, the structure of Mn_2O_3@$ZnMn_2O_4$/C microspheres still retain intact after cycling at 1000 mA g^{-1} for 700 times. Compared with the pristine electrode in Fig. S5a, the morphology after cycling shows no difference, demonstrating the high stability of the Mn_2O_3@$ZnMn_2O_4$/C microspheres. And the rod like objects in Fig. S5b are glass fiber separator stuck on electrode during cycling.

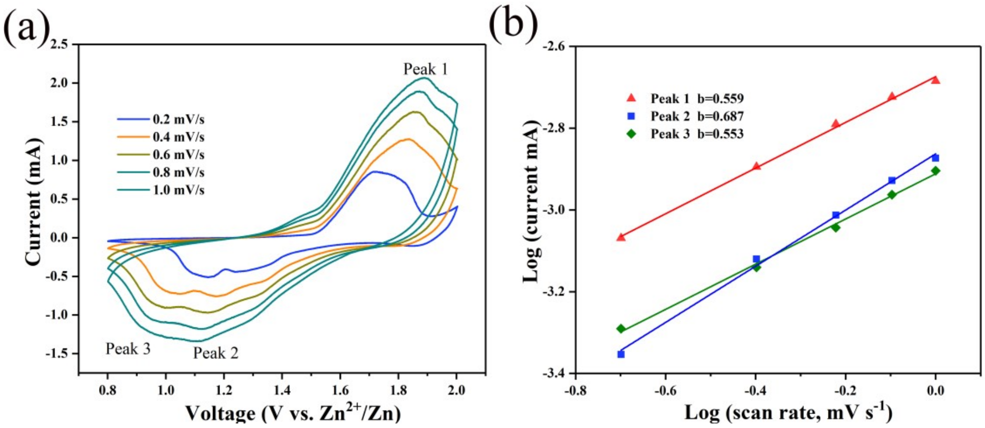

Fig. S6. (a) CV curves of Mn_2O_3@$ZnMn_2O_4$/C cathode at different scan rates; (b) Log i and log v plots at specific peak currents.